

Manuscript Details

Manuscript number	JCOMB_2018_657
Title	Design and characterisation of cellular composite structures for automotive crash-boxes manufactured by out of die ultraviolet cured pultrusion
Article type	Full Length Article

Abstract

The present paper analyses the feasibility of designing a honeycomb-like crash-box, as a cellular structure, based on data obtained from the characterisation of the building block. In order to generalise the conclusions of the study, different thicknesses and testing velocities have been analysed. The main conclusion is that, if the same thickness and testing velocity are used, the specific energy absorption (SEA) and peak load values are similar for the building block and the crash-box. Consequently, the design of the complex structure can be validated by simplifying the test procedure. However, special attention must be put on the testing velocity, since the broken fibre percentage is higher in quasi-static conditions. Thus, SEA in quasi-static tests is also higher than in the dynamic tests, 64 kJ/kg and 45 kJ/kg respectively.

Keywords	A. Glass fibres; B. Impact behaviour; D. Mechanical testing; E. Pultrusion.
Manuscript region of origin	Europe
Corresponding Author	Iván Sáenz Domínguez
Corresponding Author's Institution	University of Mondragon
Order of Authors	Iván Sáenz Domínguez, Iosu Tena, Aritz Esnaola, Mariasun Sarrionandia, JAVIER TORRE, Jon Aurrekoetxea
Suggested reviewers	Claudio Lopes, Athanasios G. Mamalis, Sivakumar Palanivelu

Submission Files Included in this PDF

File Name [File Type]

Cover letter.docx [Cover Letter]

Manuscript.docx [Manuscript File]

Figure 1.pdf [Figure]

Figure 2.pdf [Figure]

Figure 3.pdf [Figure]

Figure 4.pdf [Figure]

Figure 5.pdf [Figure]

Figure 6.pdf [Figure]

Figure 7.pdf [Figure]

Figure 8.pdf [Figure]

Figure 9.pdf [Figure]

Figure 10.pdf [Figure]

Figure Captions.docx [Figure]

Table 1.docx [Table]

Table 2.docx [Table]

Table Captions.docx [Table]

To view all the submission files, including those not included in the PDF, click on the manuscript title on your EVISE Homepage, then click 'Download zip file'.

Professor Luciano Feo
Università degli Studi di Salerno
Fisciano
Italy

Dear Prof. Feo:

I send you our work “Design and characterisation of cellular composite structures for automotive crash-boxes manufactured by out of die ultraviolet cured pultrusion” for its publication in Composite Part B: Engineering. This research is an original work that is not published elsewhere and all the authors approve the submission of the paper.

The feasibility of designing crash-box structures as a cellular component based on the building block (semi-hexagonal cross-sectioned profile manufacturing by out of die ultraviolet cured pultrusion) characterisation has been analysed. To that end, the effect of thickness and testing velocity on the energy absorption capability of the building block and the crash-box has been studied and compared.

The results show that if the same thickness and testing velocity is used, the design of the crash box based on the results of the characterisation of the building block is feasible.

Hoping that it will be of interest to be published, do not hesitate in contacting me for anything related.

Yours sincerely,

Iván Sáenz Domínguez

1st of March, 2018

Design and characterisation of cellular composite structures for automotive crash-boxes manufactured by out of die ultraviolet cured pultrusion

I. Sáenz-Domínguez ^{a*}, I. Tena ^a, A. Esnaola ^a, M. Sarrionandia ^a, J. Torre ^b, J. Aurrekoetxea ^a

^a *Mechanical and Industrial Production Department; Mondragon Unibertsitatea, Loramendi 4, 20500 Mondragón, Spain.*

^b *Irurena Group, Ctra. de Tolosa s/n, 20730 Azpeitia, Spain.*

*Corresponding author. Tel.: +34 664 256 879; e-mail: isaenz@mondragon.edu

Abstract

The present paper analyses the feasibility of designing a honeycomb-like crash-box, as a cellular structure, based on data obtained from the characterisation of the building block. In order to generalise the conclusions of the study, different thicknesses and testing velocities have been analysed. The main conclusion is that, if the same thickness and testing velocity are used, the specific energy absorption (*SEA*) and peak load values are similar for the building block and the crash-box. Consequently, the design of the complex structure can be validated by simplifying the test procedure. However, special attention must be put on the testing velocity, since the broken fibre percentage is higher in quasi-static conditions. Thus, *SEA* in quasi-static tests is also higher than in the dynamic tests, 64 kJ/kg and 45 kJ/kg respectively.

Keywords: A. Glass fibres, B. Impact behaviour, D. Mechanical testing, E. Pultrusion.

1. Introduction

In the last decades, lightweighting has become an important concern in automotive industry, aiming for a reduction of CO₂ emissions in internal combustion engines (ICE) cars and for an increased range in electric cars. However, this weight reduction must not result in a reduction of the safety of the passengers in crash scenarios. Therefore, materials with high impact energy absorption capabilities are demanded to fulfil safety and lightweighting requirements. Hence, composite materials are being widely studied for automotive applications [1]. The high specific energy absorption (SEA) capability of composite materials has been demonstrated by the research studies of many authors [2–7]. While metallic structures are designed to absorb energy by plastic deformation through progressively buckling as the column walls collapse; the absorption mechanism of composites structures is based on progressive material collapse in a brittle manner [8]. Many researchers have demonstrated that *SEA* values of composites structures are above 45 kJ/kg, depending on the geometry and the material [2,9,10]. However, a stable and progressive collapse of the composite structures has to be ensured, since the *SEA* values are dramatically reduced if the collapse is catastrophic [11].

Therefore, a progressive collapse is the first key point of a composite crash-box design. Many authors have demonstrated the importance of the geometry in the energy absorption performance of composite crash-boxes [7,12,13]. The most common geometry in real applications is the square-sectioned tubular crash structure due to assembly and integration feasibility. However, circular impact structures are the preferred cross-section from performance point of view [14]. The strategy proposed by Esnaola *et al.* [15] is an alternative solution when looking for a good compromise between integration and performance. This strategy consists of assembling semi-hexagonal profiles following a honeycomb concept. Indeed, the same semi-hexagonal profile can be used as a modular building block of a cellular composite structure [16] to fulfil different crashworthiness requirements; while the energy absorption capability of the hexagonal structures is between the circular and square tubes [14,17].

The second key point of a composite crash-box design for automotive industry is the cost effectiveness of the manufacturing process. The limited productivity of some composite manufacturing processes and the related operative costs, are an obstacle to expand the use of composites in high-volume automotive applications. Nonetheless, the out of die ultraviolet (UV) cured pultrusion has recently appeared as a new cost-effective alternative manufacturing process [18–20]. The productivity rate of this process is increased compared to the traditional pultrusion without reducing the mechanical properties of the

pultruded profiles [18]. Therefore, this process is a good candidate to manufacture crash-boxes for automotive industry in a cost effective way.

The third key point is the prediction of the energy absorption performance of the composite crash-box. It is certainly true that the response of pultruded composite tubes under axial compression has been widely investigated by many researchers [17,21]. Indeed, analysing the behaviour of the composite subjected to axial compressive loads is the most extended way to evaluate the suitability of a composite material for crashworthy applications [22]. These axial compression tests can be carried out at quasi-static and dynamic compressive conditions, but they may show different trends of the effect of impact velocity on energy absorption capability of composites [23]. In case of designing crash-boxes using honeycomb concept, the uncertainty is even higher. As the crash-box is composed by the same semi-hexagonal profile used as a building block, the key point is to probe if the energy absorption capability of this building block can be individually qualified, and as a cellular material, the periodic nature of their assemblies simplifies the analysis and prediction of their behaviour [16].

Hence, this paper deals with the prediction of the energy absorption performance of out of die UV cured pultruded crash-boxes based on the assembly of semi-hexagonal profiles (building blocks). The design process of a cellular composite crash-box is analysed, comparing the energy absorption capability of the semi-hexagonal building block and the final component at quasi-static and dynamic compression rates. The effect of parameters such as the composite thickness, impact velocity and component geometry have been analysed. It is expected that the information provided in this research study contributes to develop new guidelines on designing and characterising cellular composite crash-boxes.

2. Experimental procedure

2.1. Materials

The composite used in this study is a glass/UV cured vinyl ester composite. The reinforcement consists of 300 g/m² and 75 mm width quasi unidirectional E-glass ribbon. The reinforcement is described as quasi unidirectional because of 8% of fibres are oriented at 90° to maintain the cohesion of the unidirectional fibres. Furthermore, these fibres are interwoven with the longitudinal fibres. The resin is UV curable vinyl ester supplied by Iruena S.A., whose commercial name is IRUVIOL GFR-17 LED. The photoinitiator systems is a combination of Bis (2,4,6-trimethylbenzoyl)-phenylphosphine oxide (BAPO) and 2-Dimethylamino-2-(4-methyl-benzyl)-1-(4-morpholin-4-yl-phenyl)-butan-1-one (α aminoketone).

2.2. Specimen geometry

The basic geometry (building block) of the specimens used in this study was obtained from semi-hexagonal profiles of 1.5 mm (6 glass layers) and 2 mm (8 glass layers) of thickness (Fig. 1a). This basic geometry is used to evaluate the energy absorption capabilities of the material. Through the combination of this basic geometry, a crash-box structure can be obtained (Fig. 1b), which has demonstrated to be an optimised geometry for energy absorbing structures [15]. The assembly of the crash-box structure is based on stacking basic building blocks by adhesive joining (Hysol Loctite EA 9466[®] adhesive). In order to ensure a stable and progressive crushing of the structure and therefore to maximise the energy absorption capability, a 45° chamfer type trigger is machined in the upper side of each specimen. In this way, a progressive collapse of the specimen during the compression test will be ensured, maximizing the energy absorption capability of the composite structure [24].

Insert Fig. 1

2.3. Manufacturing process

All the specimens were manufactured by out of die UV cured pultrusion line (Fig. 1c), which has been developed entirely by the research group at Mondragon University. The impregnation was done in an open resin bath system and the pull system is a Kuka KR 180 R2500 robot arm. The pulling speed to manufacture the profiles was 0.3 m/min, which is within the range of speeds of traditional pultrusion [25]. The UV source used was a Phoseon FireFlex UV LED source (2 sources), with an emitting window of 75 × 50 mm². The maximum intensity is 8 W/cm² and the emission peak of this UV source is found at 395 nm (the composite is irradiated from both sides).

2.4. Mechanical characterisation

2.4.1. Quasi-static compression tests

Quasi-static compression tests were carried out at 10 mm/min of compression speed during 50 mm of collapse distance. The equipment used is a universal test machine, Instron 4206, equipped with 100 kN load cell. 3 specimens of each configuration were tested in order to ensure the repeatability of the tests.

Peak load, P_{\max} (kN): the maximum force of the first peak.

Mean load, P_{mean} (kN): the mean load of the collapse, equation 1.

$$P_{\text{mean}} = \frac{\int_0^{l_{\max}} P(l) dl}{l_{\max}} \quad (1)$$

where, l_{\max} (m) is the total collapsed length.

From force-displacement curve, the following crashworthiness characteristics are calculated:

Absorbed energy, A_c [kJ]: the area under load-displacement curve, equation 2.

$$A_c = \int_0^{l_{\max}} P(l)dl \quad (2)$$

Specific Energy Absorption, SEA (kJ/kg): the absorbed energy per unit of crushed specimen mass (m_t , kg), equation 3.

$$SEA = \frac{\int_0^{l_{\max}} P(l)dl}{m_t} \quad (3)$$

Crush efficiency, η_c the percentage ratio of the mean load to peak load, equation 4.

$$\eta_c = \frac{P_{\text{mean}}}{P_{\text{max}}} \cdot 100 \quad (4)$$

2.4.3. Dynamic compression tests

Two different dynamic compression tests were performed depending on the amount of energy to be dissipated by the specimen type (building block or crash-box):

The impact test for building blocks were performed using a Fractovis plus drop-weight test machine, with a mass of 35 kg for 1.5 mm thickness specimens and 45 kg for 2 mm thickness specimens. The drop height of 1 m was used (maximum permitted by the test machine) for both thicknesses. A triaxial accelerometer (PCB 356B21) was attached to the tip of the impactor to record the acceleration-time response. Hence, from acceleration-time response other impact parameters, such as displacement, velocity and load can be obtained based on the Newton's second law and kinematics [15,23].

For the case of crash-boxes, as the impact energy would be significantly higher due to the increased amount of building blocks, a different dynamic compression test was performed (Fig. 2) at Pimot facilities (Poland). In this case, an impact trolley (mass of the trolley 350 kg) has been used for the testing of the crash-boxes. The specimens have been attached on this impact trolley and impacted against a rigid wall at 37 km/h of initial impact speed. The force-displacement curves, which were needed for the calculation of the crashworthiness parameters explained before, have been obtained integrating the information recorded by the accelerometers of the trolley and from the data recorded by a high speed video camera at 10,000 frames per second.

Insert Fig. 2

2.5. Broken fibre percentage (BFP) in crushing stage

All post-crushed specimens are treated following the procedure described in ASTM D3171-09 in order to burn the matrix and analyse the post-crushing glass fibres. All broken fibres are removed leaving only those fibres which are not broken in each fibre layer. These glass fibre layers are weighed in an OHAUS GALAXY 110 electronic balance and the percentage of broken fibres within the collapsed length is calculated following the equation 5.

$$BFP = 100 \cdot \left(1 - \frac{w - \rho_L (l_T - l_C)}{\rho_L \cdot l_C} \right) \quad (5)$$

where, *BFP* is broken fibre percentage (%), *w* is the weight of the fibres that are not broken after crushing stage (g), ρ_L is linear density of glass fibre layer (g/mm), l_T is the overall length of the specimen (mm) and l_C is the collapsed length during crushing process (mm).

3. Results and discussion

3.1. Compression tests – Building block

In order to characterise the energy absorption capability and the effect of the thickness of the material at low compression speeds, building blocks were tested. Fig. 3c shows a representative load-displacement curve obtained for both analysed thicknesses, where it can be noticed that after the initial peak force, the load converges to a lower mean value. Analysing the quasi-static compression tests, it can be noticed that all the specimens had a stable and progressive crushing collapse. In addition, two images (upper and bottom view) of each specimen type are presented in Fig. 3a, 3b, 3d and 3e, where the different deformation and fracture mechanisms can be differentiated (these mechanisms have been observed in all the tested specimens, Fig. 3a and 3b):

Axial splitting between fronts, which is geometry dependant.

Axial crack propagation, where energy is absorbed spreading the axial crack progressively.

Fibre breakage.

Insert Fig. 3

Analysing the *SEA* and efficiency values of both thicknesses (Table 1), it can be stated that the energy absorption capability of the specimens is similar within the experimental scatter. Regarding the peak and mean loads, 2 mm thickness specimens present higher peak and mean load values, which is directly related to the effect of a higher resistant area (with the same fibre volume fraction). However, the dispersion of the values obtained from the 1.5 mm thickness specimens are significantly higher compared to values obtained from 2 mm thickness specimens. This fact could be due to the local buckling

phenomena noticed in some 1.5 mm thickness building blocks. The local buckling in some areas of the specimens reduces the dissipated energy, since the buckled area loses the load carrying capability. The reason for that phenomenon is the thickness of the specimen, as Mamalis *et al.* [6,26] observed in their studies; the presence of buckling areas during collapse is more common in thinner composites. This fact means that if the wall thickness is reduced above 1.5 mm, the energy absorption capacity could be significantly affected, due to local buckling effects.

In order to evaluate the effect of the crushing speed on the energy absorption capabilities of the building block, dynamic compression tests for this configuration were conducted. Fig. 4 shows three representative load-displacement curves obtained from the accelerometer data of each composite thickness.

Furthermore, as well as in quasi-static compression tests, two images (upper and bottom view) of each specimen type are presented (Fig. 4a, 4b, 4d and 4e).

Insert Fig. 4

Referred to deformation mechanisms, the same mechanisms and progressive collapse than in the quasi-static compression tests are identified in dynamic testing (the axial splitting between fronts, the axial crack propagation and fibre breakage). However, more extended delaminated areas and less fibre breakage have been identified as it is shown in Fig. 5. The building blocks tested at quasi-static compression rate present a significantly higher *BFP* (approximately 75%) compared to the building blocks tested at dynamic rates (approximately 40%). This behaviour is observed for both analysed thicknesses. The reduction of broken fibres affect directly to the energy absorption capability as it was demonstrated by Esnaola *et al.* [27,28]. Mode I collapse type is associated with large amount of energy absorbing capability (axial crack propagation and axial splitting between fronds) while Mode II collapse type is associated with low energy absorption capability (delamination between plies and flexural damage of individual plies) [29]. It can be noticed that while in quasi-static compression rates the predominant failure mode is Mode I, when the compression rate increases, the failure mode is a mixture of Mode I and Mode II. This fact is corroborated when the results of the dynamic and quasi-static compression tests are compared (Table 1). Regarding 1.5 mm thickness specimens, the *SEA* value present a significant reduction from 61.9 kJ/kg (quasi-static test) to 34.1 kJ/kg (dynamic test). A similar behaviour pattern was identified for 2 mm thickness specimens. However, in that case the reduction of *SEA* was from 65.7 kJ/kg (quasi-static test) to 43.6 kJ/kg (dynamic test). Analysing the evolution of peak and mean loads obtained from quasi-static and dynamic tests, the same behaviour was identified for both thicknesses. The

measured peak load was similar with both crushing speeds: around 14 kN for 1.5 mm thickness and 24 kN for 2 mm thickness. However, a clear reduction on the mean load was measured for both thicknesses: about 40% for 1.5 mm thickness and 35% for 2 mm thickness. This reduction is attributable to the increase of the crushing speed, which promotes the delamination between the plies rather than breaking fibres, reducing the mean collapse load, and, consequently, reducing the energy absorption capability of the material.

Insert Fig. 5

Insert Table 1

3.2. Crash-box length estimation

Based on the results obtained from the quasi-static and dynamic compression tests of building block, a estimation of the length of the crash-boxes built with 10 building blocks can be performed. In this way, the correlation between quasi-static and dynamic compression tests of building block and crash-box could be evaluated. Fig. 6 presents an estimation of the minimum crash-box length (for two crash-boxes) depending on the results from the quasi-static and dynamic compression tests. For the crash-box of 1.5 mm thickness, the minimum length can vary from 150 mm to 250 mm depending if *SEA* values are obtained from quasi-static or dynamic compression tests. The same trend is observed for 2 mm thickness, where the minimum length can vary from 100 mm to 150 mm. In order to ensure that the length of the crash-boxes will be enough for the crash-tests, the maximum estimated length should be considered. Therefore, the length of the crash-box of 1.5 mm would be 250 mm; and 150 mm for the case of 2 mm thickness. However, the length of all crash-boxes was increased in 50 mm in order to have enough free length to attach the components to the impact trolley.

Insert Fig. 6

3.3. Compression tests – Crash-box

Energy absorption capability of the crash-box at quasi-static compression rate was evaluated, as it was conducted with the building block. Regarding the quasi-static compression tests performed to crash-boxes, Fig. 7c presents a representative load-displacement curve obtained for both analysed thicknesses. In this case, as well as the building block, all the specimens had a stable and progressive crushing collapse. No differences are found in the load-displacement curve appearance (except higher values due to the combination of building blocks). Two images (upper and bottom view) of each specimen type are shown in order to analyse the deformation and fracture mechanisms (Fig.7a, 7b, 7d and 7e). Compared to

building block, the crash-box presents also high fibre breakage at quasi-static compression rate. This effect cannot be quantitatively analysed due to the size of the component and the available burner. However, through a qualitative analysis (comparing the status of the specimens after testing), the higher level of *BFP* of the crash-box is evident (all the specimens were completely broken-down). This fact may be due to that Mode I collapse type (axial crack propagation and axial splitting between fronds) is affected by the geometry of the crash-box: propagating the axial crack and splitting the fronts is hindered by the interaction with adjacent profiles. In this way, a slight decrease in *SEA* values (around 5%) is found in the crash-box (Table 2). Referred to the efficiency, as well as *SEA* value, a slight decrease is noticed in the crash-box. That effect is due to the increase of the peak load, which is slightly higher than the sum of the individual peak load of each building block. The higher stability of the crash-box increases the peak load of the component, compared to the building block. On the other hand, the local buckling issues found in 1.5 thickness building blocks are not identified in the crash-boxes.

Insert Fig. 7

In order to evaluate the effect of the crushing speed on the energy absorption capabilities of crash-boxes, dynamic compression tests were conducted. Figs 8 and 9 shows three representative load-deformation curves obtained from the accelerometer data of each composite thickness. In addition to the images of the after-crashing status of the specimens (Fig. 8c and Fig. 9c), four images of each component during the crash-test are presented (Fig. 8a and Fig. 9a). It has to be mentioned, that all the specimens had a stable and progressive collapse as it can be seen in the pictures obtained from the crash-test. Regarding the deformation mechanisms, the same mechanisms and progressive collapse than in the quasi-static compression tests are identified in dynamic testing (the axial splitting between fronts, the axial crack propagation and fibre breakage). However, as it occurs in the case of the building block at dynamic rates, broken fibre percentage gets significantly reduced compared to quasi-static compression rates. Therefore, the energy absorption capability of the component is negatively affected. This fact is corroborated analysing the values obtained from dynamic test shown in Table 2. *SEA* values are decreased from results at quasi-static rates, from approximately 60 kJ/kg to 40-45 kJ/kg within the experimental scatter (for both thicknesses). However, it has to be mentioned that the *SEA* value measured for both thicknesses at dynamic rate is similar to the values obtained from 2 mm thickness building blocks at dynamic rate. This relation can be also identified analysing the maximum collapsed lengths of the crash-boxes, which are very close with the prediction obtained from dynamic compression tests of building blocks. Regarding the

peak and mean loads, a decrease close to 30% has been measured for almost all the specimens, which is largely related to the high presence of delamination instead of fibre breakage. As in quasi-static compression test, the peak load is close to the sum of the individual peak load of each building block.

Insert Fig. 8

Insert Fig. 9

Insert Table 2

Finally, Fig. 10 shows a graphical comparison of *SEA* values obtained from quasi-static and dynamic tests for all the specimens. It can be stated, that the energy absorption capability of the tested configurations varies depending on the compression rate, being decreased at dynamic compression rates. Although some studies seems to reveal the opposite evolution of the energy absorption capability depending on the compression rate [6,26], this result is aligned with other research study recently published [23]. On the other hand, analysing the Fig. 10, it can be assumed that the estimation of the crash-box length cannot be done by quasi-static compression test, even with the same configuration of the cash-box, since the failure mode is different at higher compression rates and consequently, high differences in *SEA* values are obtained. However, it can be noticed that *SEA* values between both configurations in dynamic test are similar. Therefore, in order to design a crash-box as a cellular component, the characterisation of the building block by dynamic compression tests is needed.

Insert Fig. 10

4. Conclusions

In the present paper, a feasibility analysis of designing automotive composite crash structures as a cellular component based on the characterisation of the building block has been performed. The effect of testing velocity and thickness on the energy absorption capability has been analysed. These are the main conclusions:

The *SEA* values of the building block and the crash-boxes are similar. Furthermore, the effect of testing velocity is also the same, since *SEA* obtained from the dynamic compression tests are lower than the values from the quasi-static compression tests. This reduction can be attributed to the decrease of the mean load observed in the dynamic tests, since the change of predominant failure mechanisms, from fibre breakage in quasi-static to delamination under dynamic conditions.

Wall thickness is a critical parameter, since even using the same thickness in building blocks and crash-boxes, for thin wall designs remarkable differences can be found. The origin of the deviations is related to the fact that buckling is more probable testing the building block than in testing the crash-boxes of the same wall thickness.

The *SEA* values of building block and crash-box are similar when the characterisation is carried out with the same thickness and testing velocity, since deformation and fracture mechanisms are the same in each case. In the same way, the peak load of the crash-box can be estimated by multiplying the value of the building block and the number of units in the crash-boxes.

Taking into account the previous conclusions, the length of the crash-box can be estimated based on the *SEA* values obtained in the dynamic compression test-of the building block.

Therefore, it can be postulated that designing a crash-box composite structure as a cellular component based on the characterisation of the building blocks is feasible.

Acknowledgments

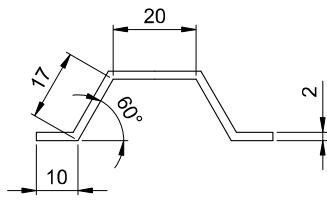
I. Saenz-Dominguez thanks the Basque Government for the grant (PRE_2015_1_0375) and for providing financial support (PUL3D UE 2015-2 & ICUV ZL-2016/00349; IT833-16; DFG) for this study. The authors also thank the European Commission for providing financial support (WEEVIL Ultralight and Ultrasafe Efficient Electric Vehicle - Grant agreement no.: 653926) for this study. Finally, the authors want to thank *Przemyslowy Instytut Motoryzacji* (PIMOT) for providing their facilities to perform the crash-tests.

References

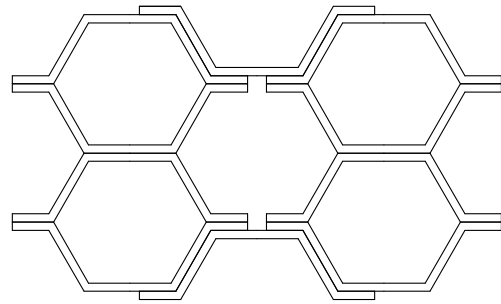
- [1] Adam H. Carbon fibre in automotive applications. *Mater Des* 1997;18:349–55.
- [2] Hull D. A Unified Approach to Progressive Crushing of Fiber-Reinforced Composite Tubes. *Compos Sci Technol* 1991;40:377–421.
- [3] Thornton PH. Energy Absorption in Composite Structures. *J Compos Mater* 1979;13:247–62.
- [4] Farley GL. Energy Absorption of Composite Materials. *J Compos Mater* 1983;17:267–79.
- [5] Carruthers JJ, Kettle AP, Robinson AM. Energy absorption capability and crashworthiness of composite material structures: A review. *Appl Mech Rev* 1998;51:635.
- [6] Mamalis AG, Manolakos DE, Ioannidis MB, Papapostolou DP. On the response of thin-walled CFRP composite tubular components subjected to static and dynamic axial compressive loading: Experimental. *Compos Struct* 2005;69:407–20.
- [7] Ochelski S, Gotowicki P. Experimental assessment of energy absorption capability of carbon-

- epoxy and glass-epoxy composites. *Compos Struct* 2009;87:215–24.
- [8] Ramakrishna S. Microstructural design of composite materials of crashworthy structural applications. *Mater Des* 1997;18:167–73.
- [9] Kakogiannis D, Chung Kim Yuen S, Palanivelu S, Van Hemelrijck D, Van Paepegem W, Wastiels J, et al. Response of pultruded composite tubes subjected to dynamic and impulsive axial loading. *Compos Part B Eng* 2013;55:537–47.
- [10] Hamada H, Ramakrishna S. Scaling effects in the energy absorption of carbon-fiber/PEEK composite tubes. *Compos Sci Technol* 1995;55:211–21..
- [11] Lau STW, Said MR, Yaakob MY. On the effect of geometrical designs and failure modes in composite axial crushing: A literature review. *Compos Struct* 2012;94:803–12.
- [12] Mamalis AG, Manolakos DE, Demosthenous GA, Ioannidis MB. Analysis of failure mechanisms observed in axial collapse of thin-walled circular fibreglass composite tubes. *Thin-Walled Struct* 1996;24:335–52.
- [13] Farely GL. Effect of specimen geometry on the energy absorption of composite materials. *J Compos Mater* 1986;20:390.
- [14] Jacob GC, Fellers JF, Simunovic S, Starbuck JM. Energy absorption in polymer composites for automotive crashworthiness. vol. 36. 2002.
- [15] Esnaola A, Ulacia I, Elguezabal B, Del Pozo de Dios E, Alba JJ, Gallego I. Design, manufacturing and evaluation of glass/polyester composite crash structures for lightweight vehicles A. *Int J Automot Technol* 2016;17:1013–22.
- [16] Cheung KC, Gershenfeld N. Reversibly Assembled Cellular Composite Materials. *Science (80-)* 2013;341:1219–21.
- [17] Palanivelu S, Van Paepegem W, Degrieck J, Van Ackeren J, Kakogiannis D, Van Hemelrijck D, et al. Experimental study on the axial crushing behaviour of pultruded composite tubes. *Polym Test* 2010;29:224–34.
- [18] Tena I, Esnaola A, Sarrionandia M, Ulacia I, Torre J, Aurrekoetxea J. Out of die ultraviolet cured pultrusion for automotive crash structures. *Compos Part B Eng* 2015;79:209–16.
- [19] Tena I, Sarrionandia M, Torre J, Aurrekoetxea J. The effect of process parameters on ultraviolet cured out of die bent pultrusion process. *Compos Part B Eng* 2016;89:9–17.
- [20] Esnaola A, Tena I, Saenz-Dominguez I, Aurrekoetxea J, Gallego I, Ulacia I. Effect of the manufacturing process on the energy absorption capability of GFRP crush structures. *Compos Struct* 2018;187:316–24.
- [21] Othman A, Abdullah S, Ariffin AK, Mohamed NAN. Investigating the quasi-static axial crushing behavior of polymeric foam-filled composite pultrusion square tubes. *Mater Des* 2014;63:446–59.
- [22] Ramakrishna S. Energy absorption behaviors of knitted fabric reinforced composite tubes. *J Reinf Plast Compos* 1995;14:1121–41.
- [23] Liu Q, Ou Z, Mo Z, Li Q, Qu D. Experimental investigation into dynamic axial impact responses of double hat shaped CFRP tubes. *Compos Part B Eng* 2015;79:494–504.
- [24] Farley GL. Energy absorption of composite material and structure 1987.
- [25] Suratno BR, Ye L, Mai YW. Simulation of temperature and curing profiles in pultruded composite rods. *Compos Sci Technol* 1998;58:191–7.
- [26] Mamalis AG, Manolakos DE, Demosthenous GA, Ioannidis MB. The static and dynamic axial collapse of fibreglass composite automotive frame rails. *Compos Struct* 1996;34:77–90.

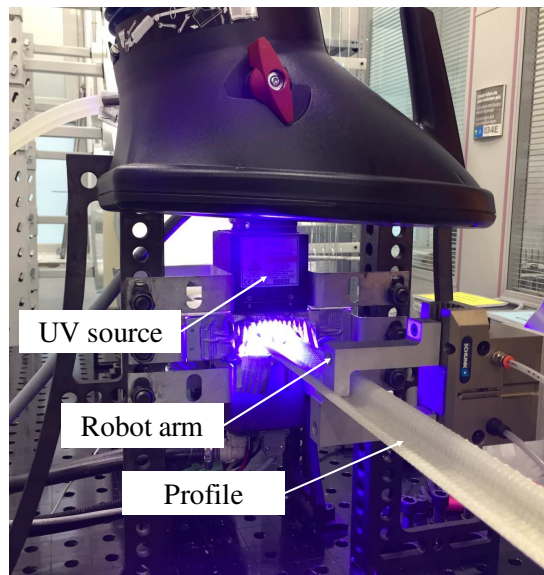
- [27] Esnaola A, Ulacia I, Aretxabaleta L, Aurrekoetxea J, Gallego I. Quasi-static crush energy absorption capability of E-glass/polyester and hybrid E-glass-basalt/polyester composite structures. *Mater Des* 2015;76:18–25.
- [28] Esnaola A, Tena I, Aurrekoetxea J, Gallego I, Ulacia I. Effect of fibre volume fraction on energy absorption capabilities of E-glass/polyester automotive crash structures. *Compos Part B Eng* 2016;85:1–7.
- [29] Hadavinia H, Ghasemnejad H. Effects of Mode-I and Mode-II interlaminar fracture toughness on the energy absorption of CFRP twill/weave composite box sections. *Compos Struct* 2009;89:303–14.



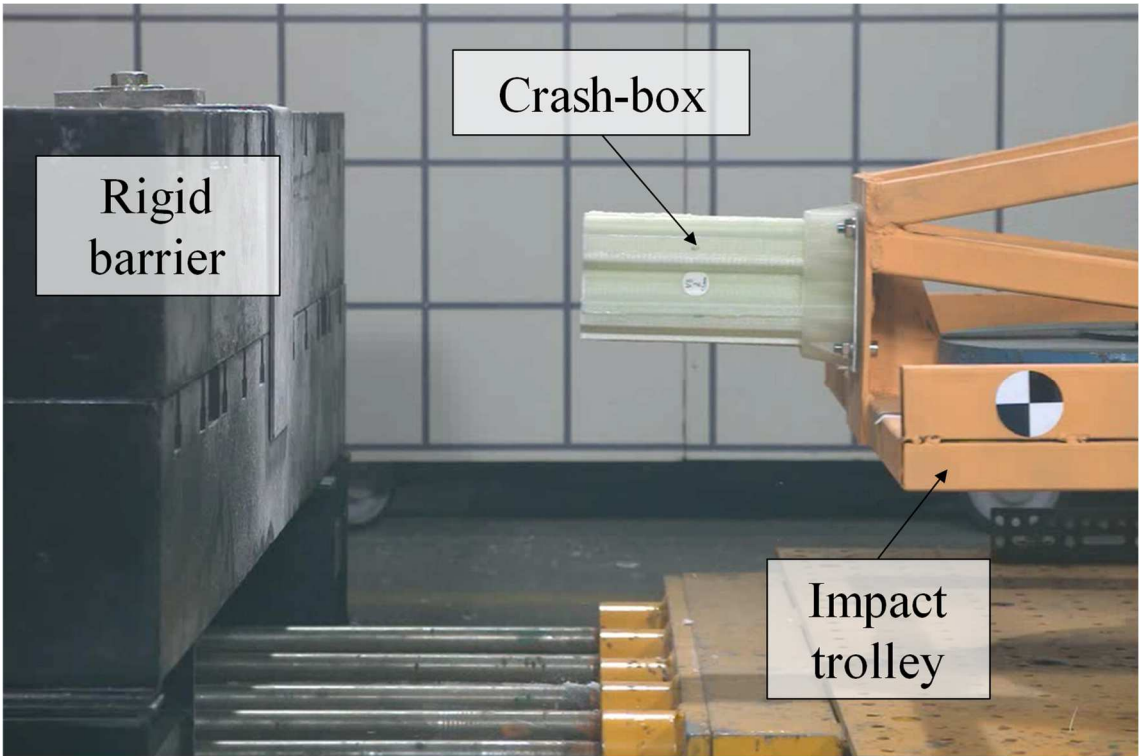
(a)

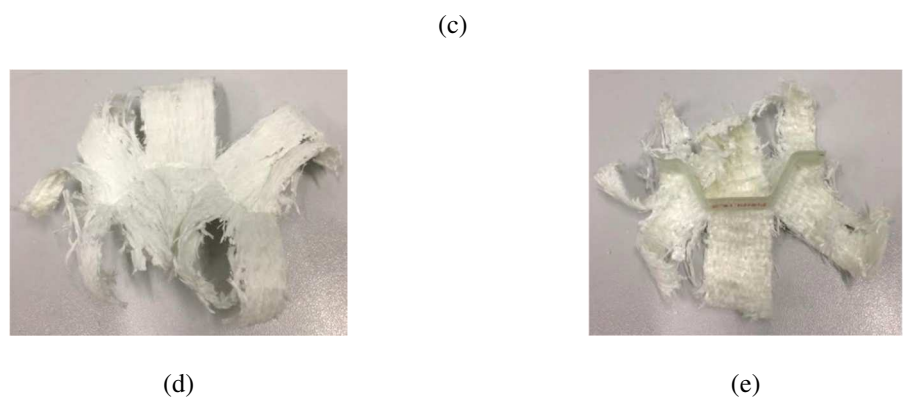
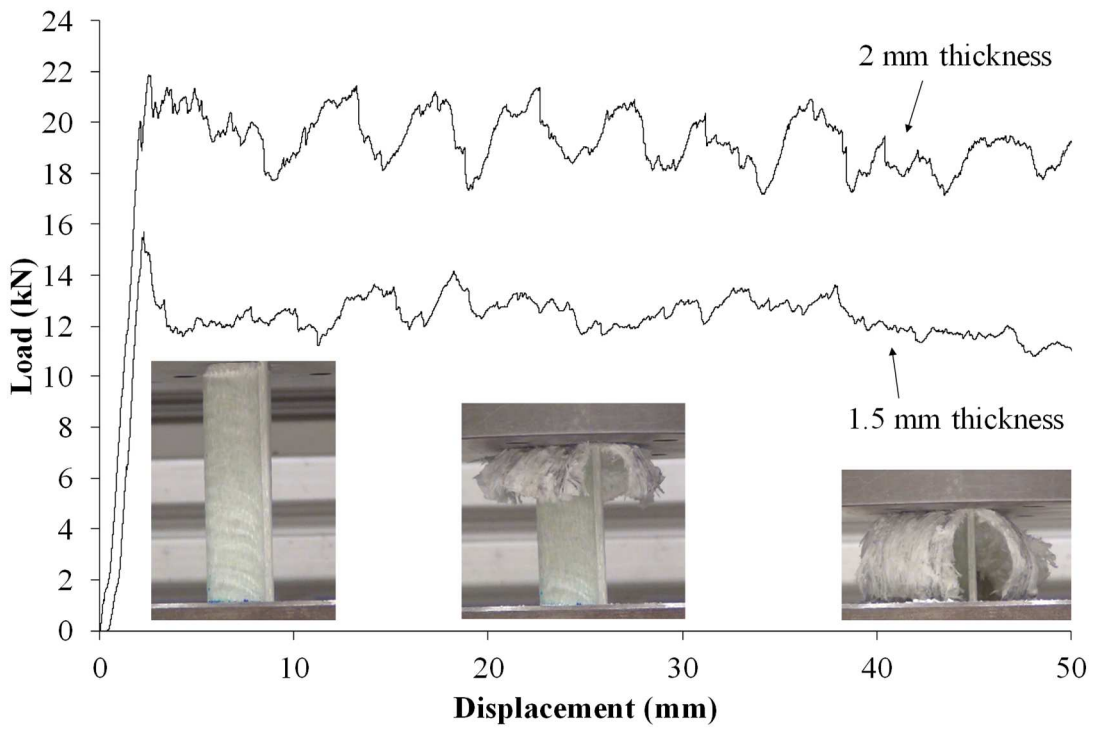
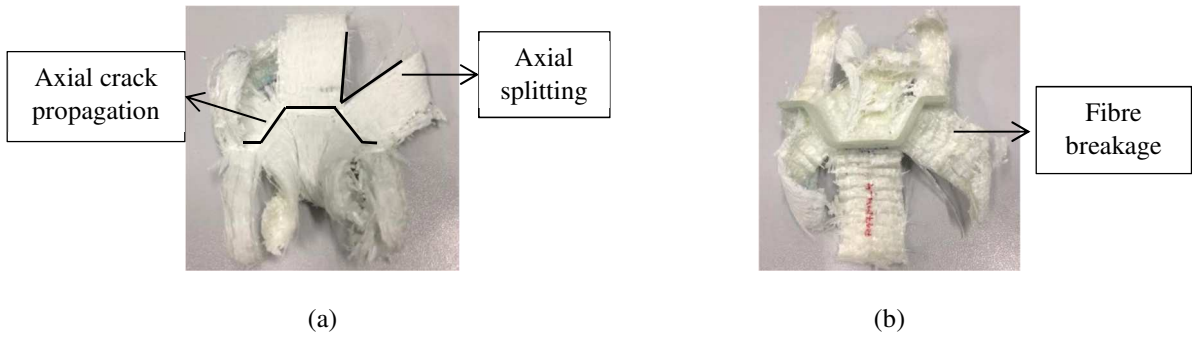


(b)



(c)



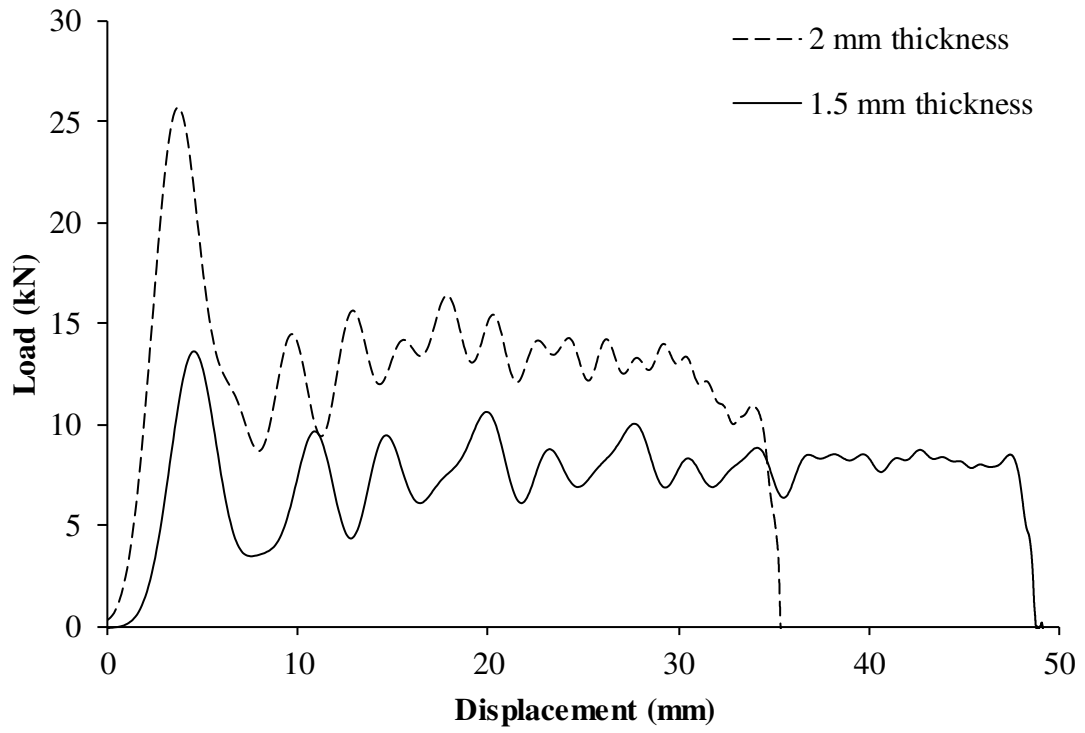




(a)



(b)



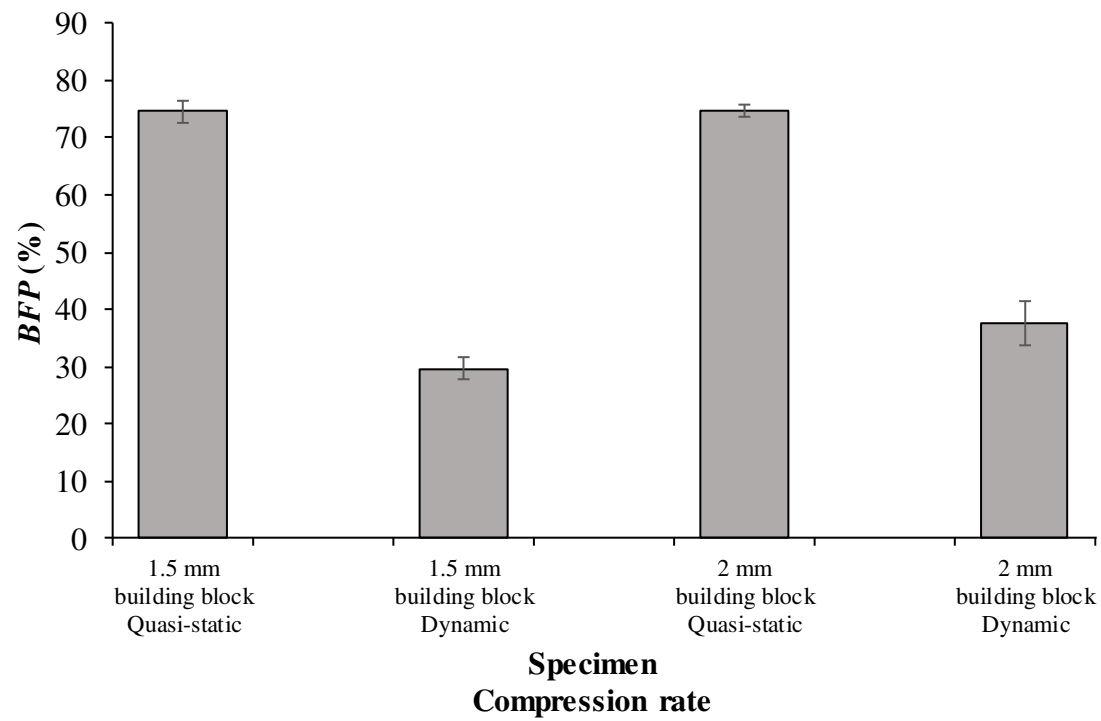
(c)

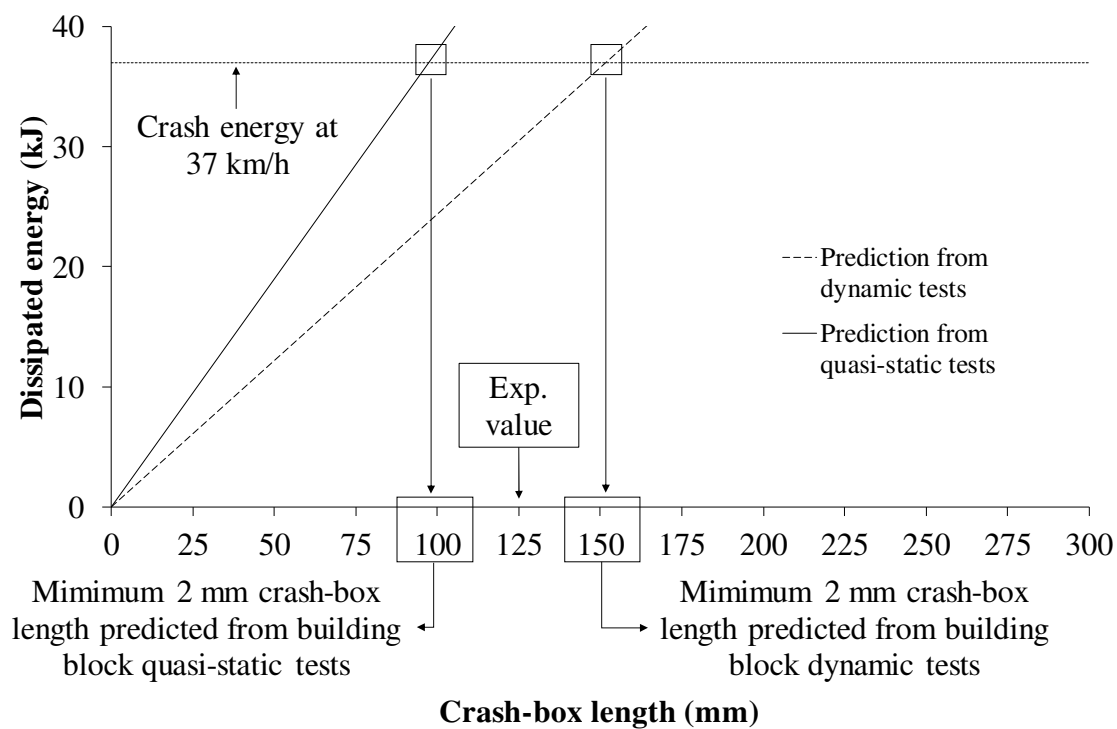


(d)

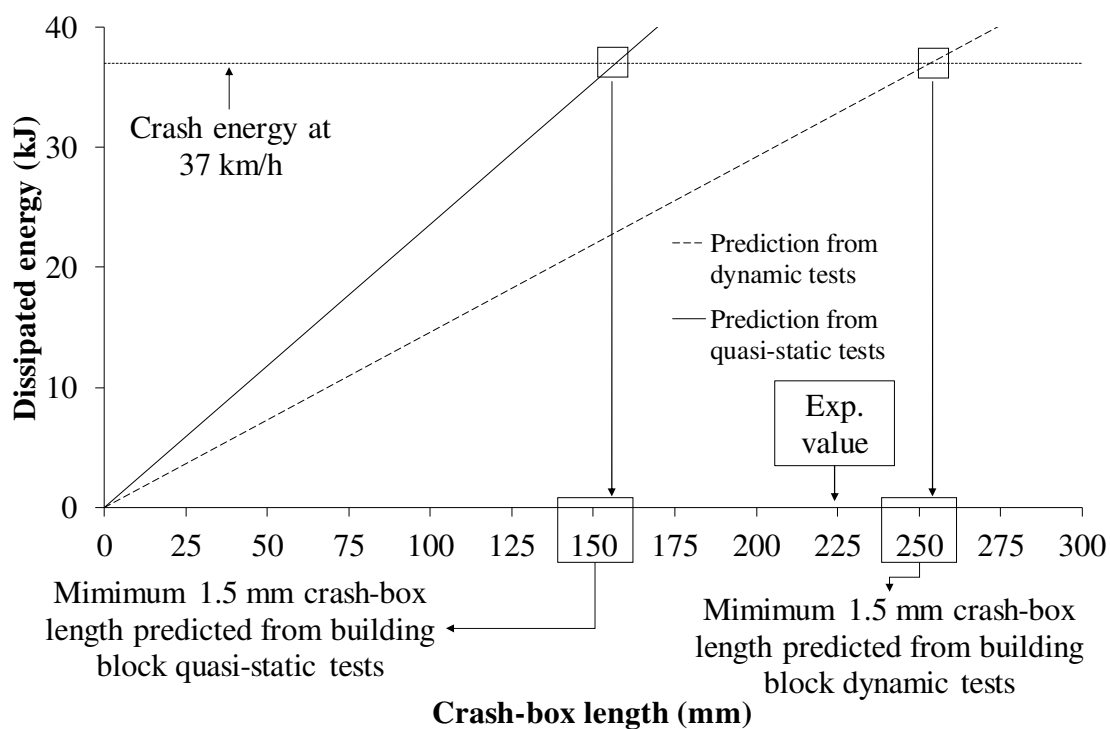


(e)





(a)



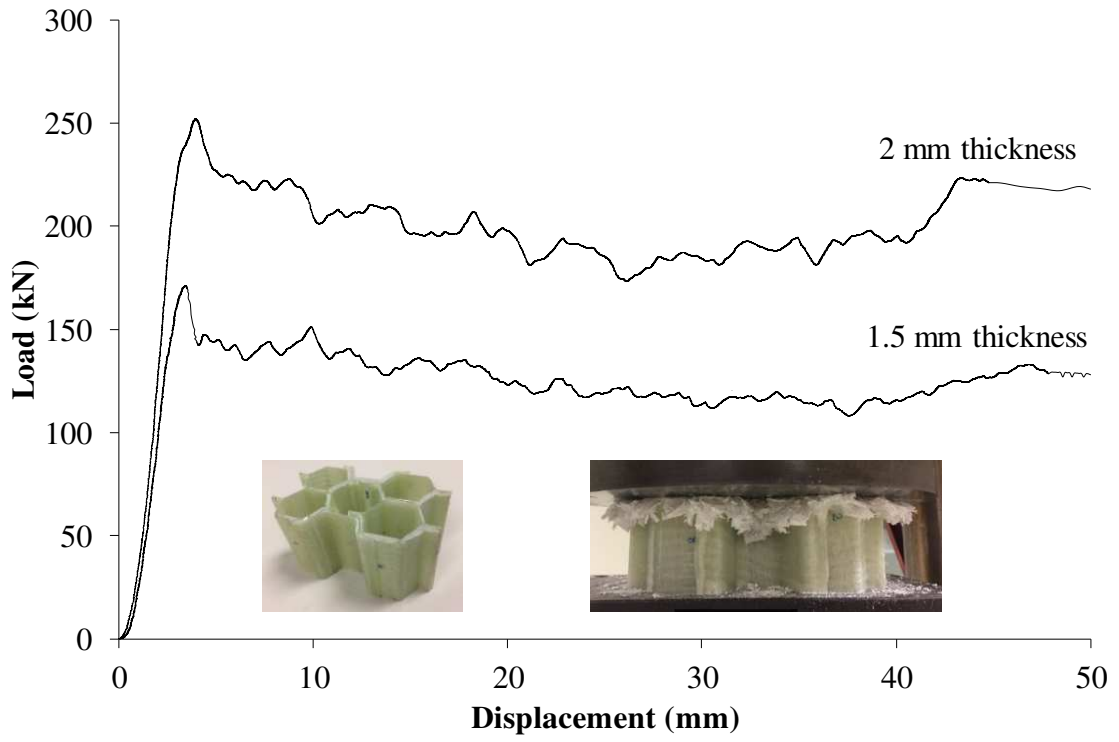
(b)



(a)



(b)



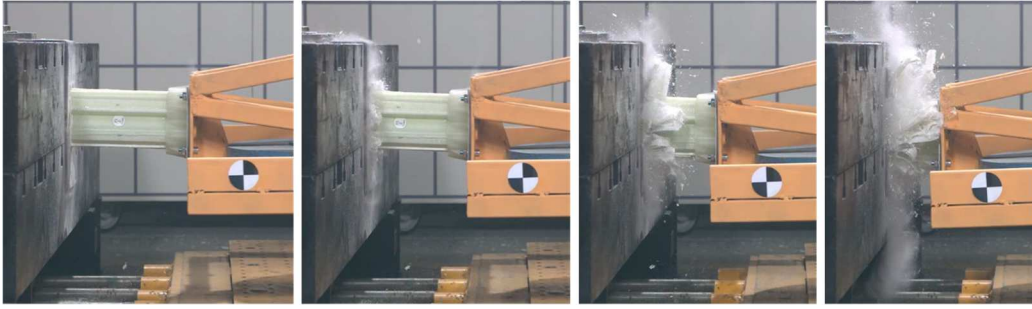
(c)



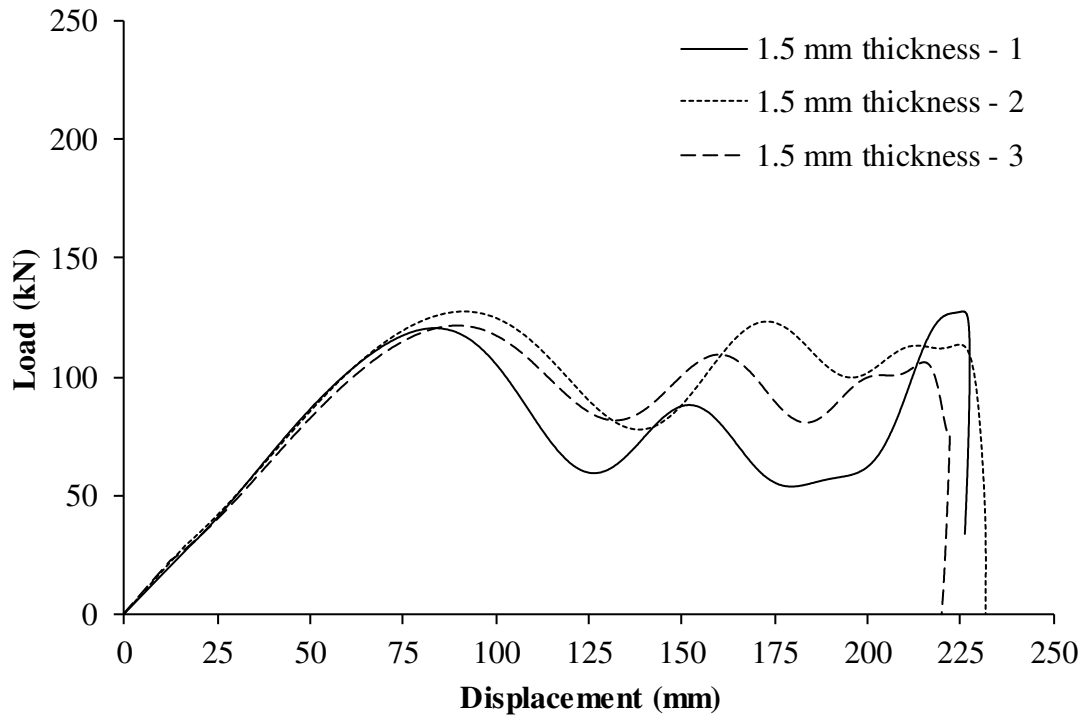
(d)



(e)



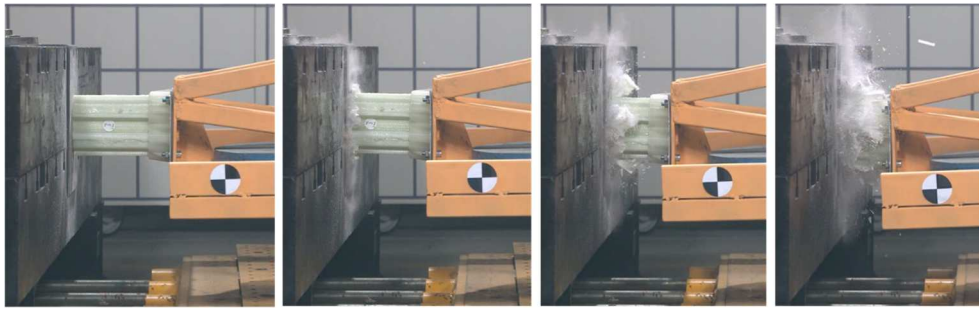
(a)



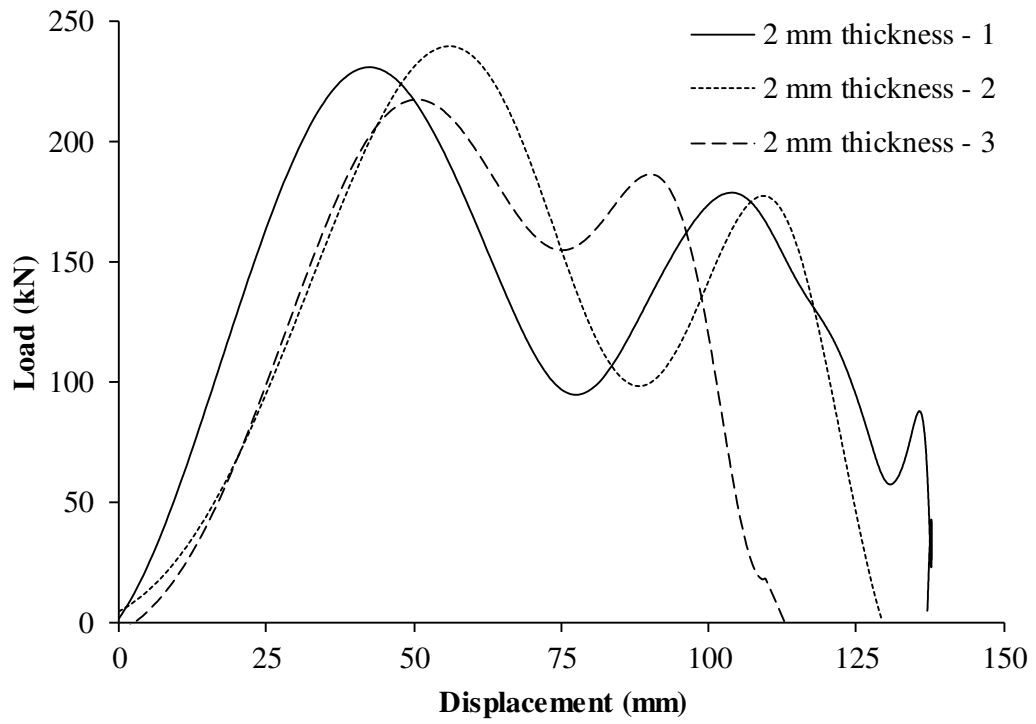
(b)



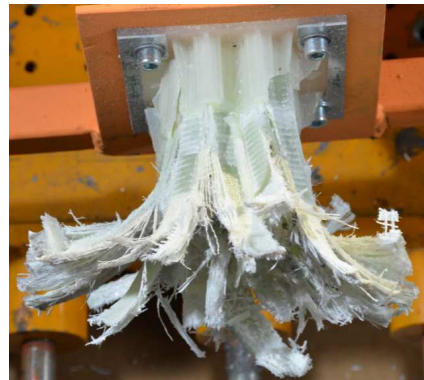
(c)



(a)



(b)



(c)

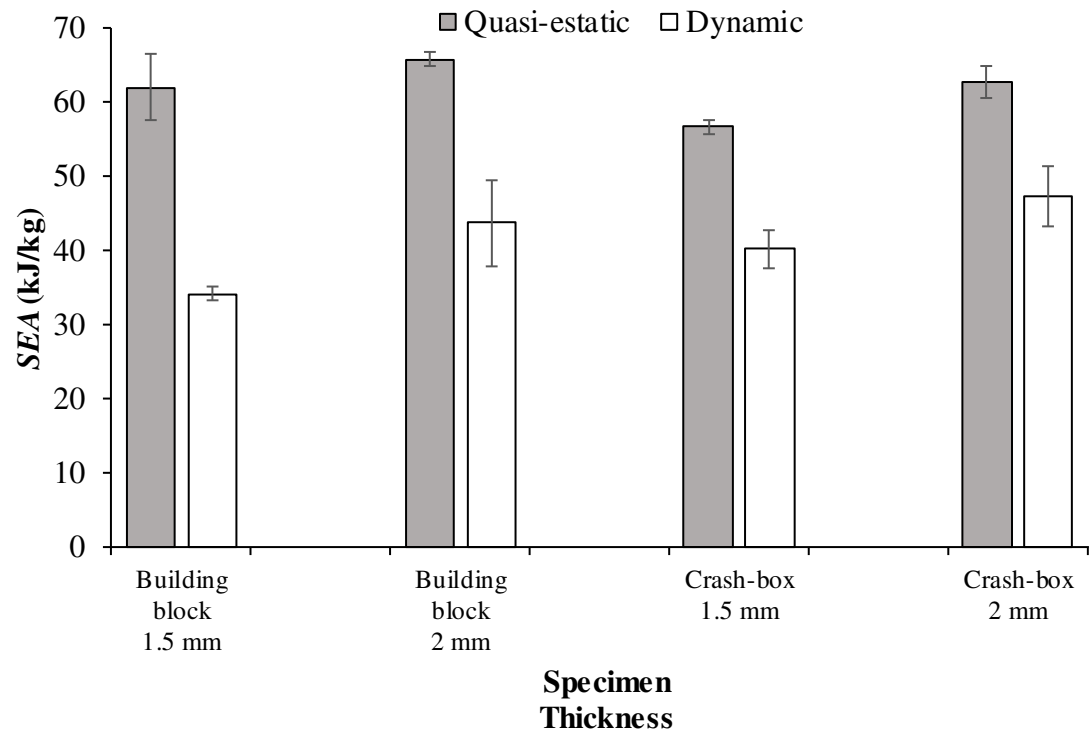


Fig. 1. (a) Building block cross-section; (b) Crash-box cross-section; (c) Out of die UV cured pultrusion machine detail.

Fig. 2. Crash-test of crash-box specimens at PIMOT facilities.

Fig. 3. (a) 2 mm thickness building block after quasi-static compression test (upper view); (b) 2 mm thickness building block after quasi-static compression test (bottom view); (c) representative load displacement curve of quasi-static compression test; (d) 1.5 mm thickness building block after quasi-static compression test (upper view); (e) 1.5 mm thickness building block after quasi-static compression test (bottom view).

Fig. 4. (a) 1.5 mm thickness building block after dynamic compression test (upper view); (b) 1.5 mm building block thickness after dynamic compression test (bottom view); (c) load displacement curves from dynamic compression test of 1.5 mm thickness and 2 mm thickness building blocks; (d) 2 mm thickness building block after dynamic compression test (upper view); (e) 2 mm thickness building block after dynamic compression test (bottom view).

Fig. 5. Comparison of different BFP of specimens tested in quasi-static and dynamic conditions.

Fig. 6. Estimation of the minimum crash-box length: (a) 1.5 mm of thickness; (b) 2 mm of thickness.

Fig. 7. (a) 2 mm thickness crash-box after quasi-static compression test (upper view); (b) 2 mm thickness crash-box after quasi-static compression test (bottom view); (c) Load-displacement curves of crash-boxes from dynamic compression test; (d) 1.5 mm thickness crash-box after quasi-static compression test (upper view); (e) 1.5 mm thickness crash-box after quasi-static compression test (bottom view).

Fig. 8. (a) Dynamic compression test sequence of 1.5 mm thickness crash-boxes; (b) Load-displacement curves of 1.5 mm thickness crash-boxes from dynamic compression test; (c) 1.5 mm thickness crash-box after dynamic compression test.

Fig. 9. (a) Dynamic compression test sequence of 2 mm thickness crash-boxes; (b) Load-displacement curves of 2 mm thickness crash-boxes from dynamic compression test; (c) 2 mm thickness crash-box after dynamic compression test.

Fig. 10. Results from quasi-static and dynamic tests for all the specimens

Configuration	Specimen thickness (mm)	Compression rate	Energy absorption capability				Failure Mode
			<i>SEA</i> (kJ/kg)	<i>P</i> _{max} (kN)	<i>P</i> _{mean} (kN)	<i>η</i> _c (%)	
Building block	1.5	10 mm/min	61.9 ± 4.4	14.8 ± 2.0	11.8 ± 0.8	76 ± 6	I
Building block	2	10 mm/min	65.7 ± 0.9	21.9 ± 0.2	18.6 ± 0.2	85 ± 1	I
Building block	1.5	15 km/h	34.1 ± 1.0	13.4 ± 0.3	7.2 ± 0.4	54 ± 2	I, II
Building block	2	15 km/h	43.6 ± 1.9	24.2 ± 1.5	12.2 ± 1.6	51 ± 5	I, II

Configuration	Specimen thickness (mm)	Compression rate	Energy absorption capability				Failure Mode
			<i>SEA</i> (kJ/kg)	<i>P</i> _{max} (kN)	<i>P</i> _{mean} (kN)	<i>η</i> _c (%)	
Crash-box	1.5	10 mm/min	56.6 ± 1.0	175.0 ± 5.0	123.7 ± 12.7	71 ± 5	I
Crash-box	2	10 mm/min	62.7 ± 2.2	258.4 ± 8.0	195.7 ± 3.0	75 ± 2	I
Crash-box	1.5	37 km/h	40.1 ± 2.6	123.3 ± 4.2	86.3 ± 9.3	69 ± 8	I, II
Crash-box	2	37 km/h	47.2 ± 4.1	229.5 ± 9.7	131.5 ± 5.3	57 ± 3	I, II

Table 1. Results of building block compression tests.

Table 2. Results of crash-box compression tests.